Transportation Infrastructure Geotechnology (2024) 11:3695–3713
https://doi.org/10.1007/s40515-024-00448-w

TECHNICAL NOTE

Effective Utilization of Stone Powder in Road Construction Using Sandwich Technique: A Laboratory Study

Eswara Reddy Orekanti[1,3] · **Venkatesh Buragadda**[1,2] · **Sai Dharani Salammagari**[1] · **Guru Swathi Vallepu**[1]

Accepted: 22 July 2024 / Published online: 9 August 2024

Abstract

A series of California Bearing Ratio (CBR) tests were performed on unreinforced and reinforced roads using natural woven jute geotextile (JGT) and woven polypropylene geotextile (PGT) reinforcements. Three different sands were used to understand the influence of sand-geotextile interface frictional properties on the optimum sand layer thickness (t). The CBR test results on reinforced (non-sandwich) conditions showed the optimum depth of JGT and PGT reinforcements are 0.4 times and 0.5 times the size of the loading plate, respectively. The improvement does not show any significant variation as compared to unreinforced conditions. Also, the test results showed the load-carrying capacity for the case of the sandwich condition increased to more than 1.3 times to 3.5 times depending upon the interface frictional properties of sand-geotextile. Based on the test conditions, the optimum thickness range of sand layers for all encapsulated reinforcement cases is determined. The test results proved the sand-geotextile interface frictional properties influenced the optimum thickness of encapsulated sand layers and the extent of improvement.

Keywords CBR tests · Geotextile · Interface properties · Stone powder · Sandwich technique

1 Introduction

In the past few years, several researchers focused on the utilization of by-product industrial waste such as fly ash and pond ash used as filling material and especially for road constructions (Bera et al. 2007; Ghosh 2010; Sarkar and Dawson 2015; Pradhan and Pothal 2024a, b; Kedar et al. 2024). In general, granite and stones are cut into smaller blocks to achieve the correct shape and size. Thirty percent of the original stone or granite mass is lost as powder (called stone powder) during the cutting process. Annually, the stone powder generates a quarrying waste of 175 million

Extended author information available on the last page of the article

tons throughout the world. As a result, large tracts of land are required to store stone powder, and disposing of this stone powder as waste poses environmental risks and difficulties (Liu et al. 2022). As per the literature, a few researchers proved the effective utilization of stone powder for the improvement of index and engineering geotechnical properties of expansive soils (Blayi et al. 2021; Teferra et al. 2023). Blayi et al. (2021) test results proved adding 40% rock powder to expansive soil samples could result in a 40% reduction in the road sub-base thickness. However, the research studies related to the behavior of stone powder as a road construction material using geosynthetics have not received much attention from the researchers.

In reinforced soil structures, the efficient operation of reinforcement mostly depends on the mobilization of interfacial shearing resistance between the soil and reinforcement (Sridharan et al. 1991; Yetimoglu et al. 1994; Ghosh et al. 2005; Roy et al. 2019; Buragadda et al. 2024). Stone powder is a waste type of powdery solid material comprised of non-plastic fines. Hence, the frictional properties of stone powder may not be as prominent as sand. The sandwich method involves placing thin layers of sand on both sides of the reinforcement (i.e., within backfill soil) to enhance the interface frictional properties. Based on the experiments performed by various researchers revealed that providing more than optimum sand layer thickness does not improve any further soil-geosynthetic interactions (Sridharan et al. 1991; Abdi et al. 2009; Yang et al. 2015). Unnikrishnan et al. (2002) carried out small-scale triaxial (UU) tests on sandwich conditional soil using different kinds of reinforcement materials such as woven geotextile, non-woven geotextile, and micro-grid. The test results proved that the optimum thickness of the sand layer is 8 mm for the higher confining pressures (> 100 kPa) and 15 mm for the lesser confining pressures. It could be due to the high soil-reinforcement interactions at lesser confining pressures (Abdi and Arjomand 2011). Contrastingly, Yang et al. (2015) found that the optimum thickness is 10 to 15 mm (for confining pressures < 100 kPa) and 15 to 20 mm (for confining pressures > 100 kPa) from the triaxial (UU) tests. The contradictory results might have occurred due to variations in the properties of reinforcement material and interfacial properties in the cases of Unnikrishnan et al. (2002) and Yang et al. (2015). Similarly, Abdi et al. (2009) performed direct shear tests using uniaxial geogrids which enclosed by less frictional kaolin and different thicknesses of cohesionless soils of 4 to 14 mm with an equivalent incremental difference of 2 mm. The test results proved that the optimum thickness (i.e., 10 mm) of the sand layer is independent of applied confining pressures. Moreover, the pullout resistance decreases after the optimum sand layer thickness, irrespective of confining pressure (Abdi and Arjomand 2011). Similar kinds of pullout tests were performed on large-scale laboratory model tests by Abdi and Zandieh (2014) and showed the optimum thickness of the sand layer is 80 mm, irrespective of confining pressure. This value is 8 times higher than the optimum value obtained by Abdi and Arjomand (2011) under the same pullout tests. It might have happened due to variations in the reinforcement materials, the size of the pullout test model, and the properties of backfills. As per the authors' knowledge, no studies have been performed to understand the influence of sand-geosynthetic interface frictional properties on the optimal sand layer thickness in the sandwich technique.

Based on the above discussions, the present study mainly focuses on the utilization of stone powder in road constructions or backfills by sandwich technique. Moreover, this research also attempts to examine the effect of interface frictional properties of sand which encapsulates geotextile in sandwich technique on the optimum sand layer thickness and improvement of load-carrying capacity.

2 Test Materials

2.1 Sand

In the present study, three different types of cohesionless sands named S1, S2, and S3 were used. The soil S1 was collected from the Swarnamukhi River (nearer to the institute), Tirupati, Andhra Pradesh, India. The soils S2 and S3 were procured from M/S Chirala Traders located in Kadavakuduru Village, Chirala, Andhra Pradesh, India. The photographic view of all three S1, S2, and S3 is depicted in Fig. 1. The soil dry sieve analysis was performed as per ASTM D6913-17, and the respective size distribution graphical plot is shown in Fig. 2. According to the USCS classification system, all three sands are classified as poorly graded sand (SP). Further, the sand index and engineering properties were also determined as per ASTM standards and mentioned in Table 1.

2.1.1 Stone Powder

Stone powder is a by-product substance that is produced in stone-cutting plants during building stone cutting and shaping. In this process, the water is used for cooling up the cutting saw; hence, the stone powder is mixed with water and flows out as stone slurry. Stone slurry is a highly viscous liquid consisting of extremely small and suspended particles. Hence, the collected stone slurry was oven-dried and sieved. The stone slurry was collected from Vijaya Granites Pvt Ltd., Tirupati (near Renigunta road), Andhra Pradesh, India. The stone powder sieve analysis was performed as per the ASTM D6913-17 and ASTM D7928-21. The corresponding particle size

Fig. 1 Photographic view of soil samples used in the present study

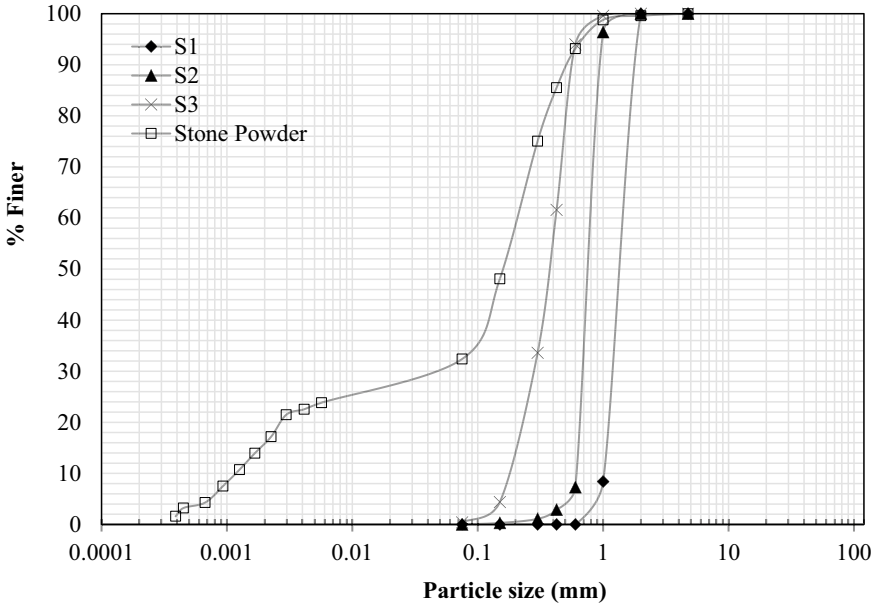

Fig. 2 Particle size distribution curves of test soils of the present study

Table 1 Properties of test soils used in the present research

Properties	Results			
	S1	S2	S3	Stone powder
Specific gravity, Gs	2.66	2.61	2.63	2.52
Grain size distribution (%)				
Gravel	0	0	0	0
Sand	100	100	100	68
Fines	0	0	0	32
D_{10} (mm)	0.96	0.6	0.17	0.02
D_{30} (mm)	1.25	0.67	0.28	0.06
D_{50} (mm)	1.4	0.77	0.37	0.16
D_{60} (mm)	1.5	0.8	0.41	0.21
C_u	1.56	1.33	2.42	9.34
C_c	1.08	0.93	0.02	0.72
Unified soil classification symbol (USCS)	SP	SP	SP	SM
Liquid limit (%)	-	-	-	27.7
Optimum moisture content (%)	-	-	-	18
Maximum dry unit weight (kN/m^3)	16.5	16.4	16.9	17.24
Minimum dry unit weight (kN/m^3)	14.9	14.34	14.7	-
Maximum void ratio (e_{max})	0.821	0.817	0.821	-
Minimum void ratio (e_{min})	0.838	0.840	0.844	0.853
Dry unit weight corresponding to 70% relative density (kN/m^3)	16	15.73	16.2	-

distribution is shown in Fig. 1. The corresponding percentage of particle sizes is mentioned in Table 1. According to the Unified Soil Classification System (USCS), the stone powder soil is classified as silty sand (SM). Several tests known as a liquid limit, non-plastic material specific gravity, and proctor tests for dry density were performed as per ASTM standards and the respective test results are also mentioned in Table 1. The modified proctor compaction tests were performed as per ASTM D1557-12, and the corresponding maximum dry unit weight and optimum moisture content are determined and enumerated in Table 1.

2.1.2 Jute and Polypropylene Geotextiles

The natural woven jute and synthetic woven polypropylene geotextiles were used as reinforcement materials in the present study as depicted in Fig. 3a. The jute geotextile (JGT) was procured from the National Jute Board (NJB) approved company,

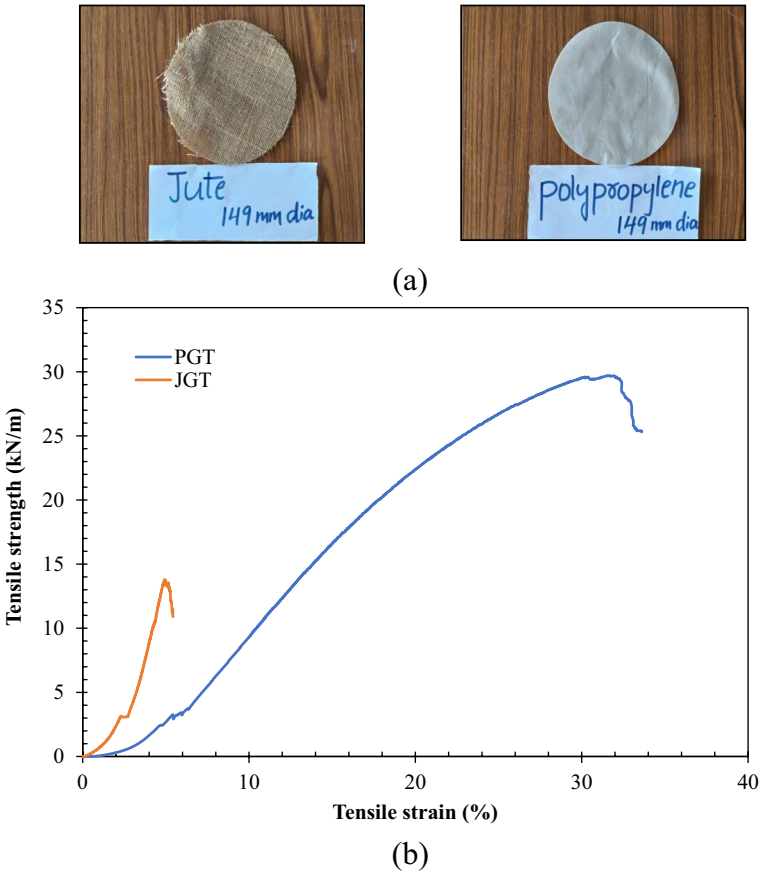

Fig. 3 Reinforcement materials used in the present study: **a** Photographic view. **b** Tensile strength–strain plots

M/s. Ballyfabs International Ltd., Chennai, India. The polypropylene geotextile (PGT) was collected from M/S Techno Fabrics Geosynthetic (P) Ltd., Gujarat, India. The physical and mechanical properties of JGT and PGT were determined based on ASTM standards as depicted in Table 2. The wide-width tensile strength tests were performed as per ASTM D4595-17 at a strain rate of 10 mm/min. The corresponding tensile strength–strain graphical plot is presented in Fig. 3b.

The soil-geotextile interface shear strength properties were determined using a direct shear test box having a size of 60 mm × 60 mm × 30 mm. Sand was poured to the relative density of 70% inside the top and bottom parts of a shear box and placed the geotextile at the interfaces of the top and bottom halves. Thereafter, the upper shear box allowed to move over the placed geotextile specimen at a strain rate of 1.25 mm/min (Latha et al. 2024; Venkateswarlu et al. 2023a, b). The shear load and horizontal displacement were continuously measured using a load cell and a horizontal dial gauge, respectively. The measured shear load and the geotextile contact area with the sand were used to compute the shear stress. Each test was performed under three distinct normal stresses of 50 kPa, 100 kPa, and 150 kPa. The corresponding stone powder–geotextiles and sands-geotextile interface shear strength properties are mentioned in Table 3.

2.2 Experimental Procedure

A series of laboratory CBR tests were conducted in the present study on the unreinforced and reinforced stone powder specimens. As per ASTM D1883-21, the tests were carried out inside a modified proctor mold in an unsoaked condition. Due to the hydrophilic nature of JGT, the physical (thickness, mass per unit area, and size of openings) and mechanical properties (tensile stiffness/strength) of jute geotextile vary in the case of soaked conditions. Hence, the present study model tests were limited to unsoaked conditions. Similar kinds of model tests were found in the literature carried out by Yetimoglu et al. (2005). The mold was a stiff metal cylinder that measured 178 mm in height and 152 mm in internal diameter. The automated

Table 2 Properties of reinforcement materials used in the present research

Property	Standards	*JGT*	*PGT*
Physical properties			
Thickness (mm)	ASTM D5199-12	1	0.4
Mass per unit area (g/m^2)	ASTM D5261-10	315	130
Mechanical properties			
Ultimate tensile strength (kN/m)	ASTM D4595-17		
Machine direction		13.8	29.6
Cross-machine direction		12.5	23.5
Failure strain-MD x CMD (%)			
Machine direction		4.9	30.2
Cross-machine direction		5.9	21.4
Secant modulus (tensile stiffness), *EA* at 5% strain (kN/m)		246	101

Table 3 Interface properties of soil-reinforcements

Soil type	Internal properties		Interface properties			
	c (kPa)	ϕ (deg)	PGT		JGT	
			c_{int} (kPa)	ϕ_{int} (deg)	c_{int} (kPa)	ϕ_{int} (deg)
Stone powder	0.72	27.04	0.2	22.30	0.31	24.06
S1	0	35.75	0	30.70	0	31.55
S2	0	33.02	0	28.35	0	30.77
S3	0	32.30	0	26.75	0	32.34

loading machine consists of a calibrated 5 T proving ring that was utilized to run the 50-mm penetration piston (D). The loading machine had a moveable base that moved at a constant strain rate of 1.27 mm/min. The loads were meticulously recorded with the penetration of piston diameter (D) of 50 mm in each series of tests. As per the protocol of ASTM D 1557-12, the test specimens were compacted in the mold using a modified proctor at an optimum moisture content and maximum dry unit weight (Table 1). The soil is compacted into five layers by applying 55 blows to each layer with a 4.89 kg hammer that is dropped from a height of 45 cm. A similar procedure was followed in the case of reinforced conditions of both normal and sandwich cases. Figure 4 shows the complete schematic view and photographic views of the CBR test setup.

2.3 Experimental Program

Table 4 shows the complete testing program adopted in the present research. Series A model tests were performed on unreinforced stone powder at maximum dry unity weight and optimum moisture content conditions. Thereafter, to determine the reinforcement effect on the improvement of CBR, the reinforcement materials of jute geotextile (JGT) and polypropylene geotextile (PGT) placed at different placement depths (u) from the surface of a soil sample as shown in Fig. 4a. Series B, Series C, and Series D model tests represent the effect of the sandwich technique on the improvement of CBR (Fig. 4b). Series B, Series C, and Series D tests were performed to find out the optimum thickness of sand layers (t) and corresponding sand layers thickness effect on the improvement of CBR load by varying sand properties using S1, S2, and S3, respectively. The amount of sand thickness (t) varied in each test series is also enumerated in Table 4.

3 Results and Discussion

3.1 Unreinforced and Reinforced Conditions

Initially, the CBR tests were performed on unreinforced conditions of stone powder at maximum dry unit weight and optimum moisture content. Thereafter, the tests were performed using JGT and PGT reinforcements by placing them at different placement depths from the plunger surface of the mold (u). Irrespective of the

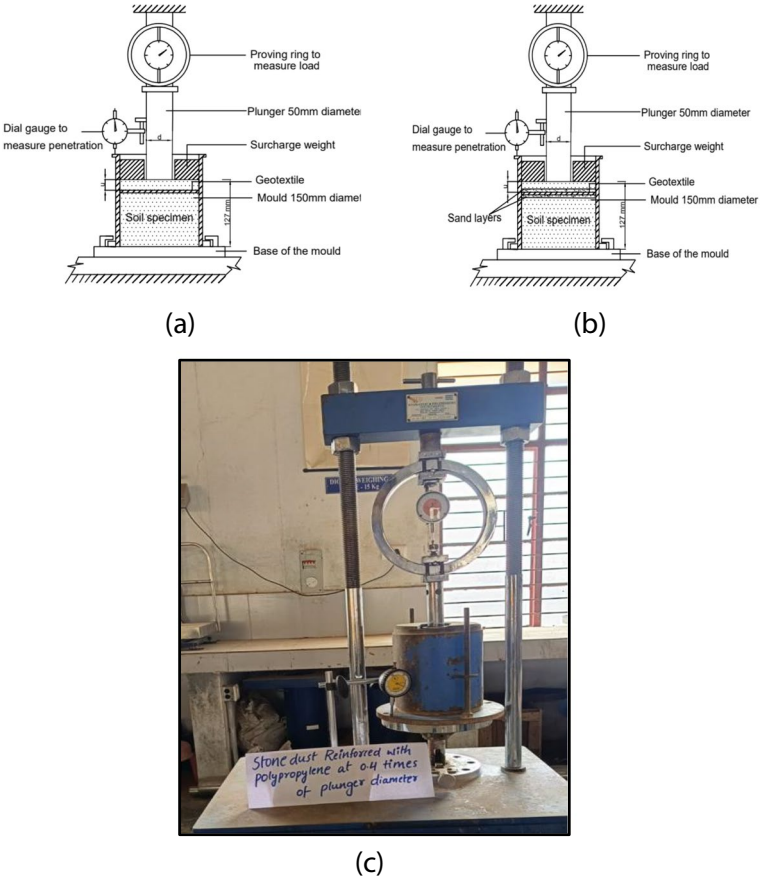

Fig. 4 Laboratory CBR test set up along with test sample: **a** Schematic view of reinforced soil sample. **b** Schematic view of reinforced soil encapsulated by sand sample. **c** Photographic view

reinforcement, the depth of the reinforcement layers was varied to 0.2D, 0.3D, 0.4D, and 0.5D (D is plunger diameter of 50 mm). Figures 5 and 6 depict the variation of load penetration of stone powder with jute and polypropylene reinforcement layers of different placement depths (u). Figure 6 graphical plots show a concave upward variation in the initial portion of the curve for different cases. It might occur due to the lesser soil-geotextile interactions and confinement in the initial loadings. Hence, the correction is applied for all the tests by expanding the tangent at the steepest point on the experimental curve and projecting it downward to intersect the penetration axis, irrespective of reinforcement and encapsulated sand. Improvement factor (IF) was used to understand the influence of depth of reinforcement layer (u) on the CBR load increment. The improvement factor is the ratio of load-carrying capacity corresponding reinforced condition to the unreinforced conditional state of soil at the same penetration depth. Figure 7 depicts the variation of the improvement factor of reinforced stone powder of JGT and PGT under different placement depths

Table 4 Testing program of the present research

Series designation	Geometrical parameters of reinforcement layers		Objective of the series
	Variable	Constant	
A	-	-	Tests on unreinforced stone powder
	$u=0.2D$ $u=0.3D$ $u=0.4D$ $u=0.5D$	JGT PGT	For determination of optimum depth of reinforcement in the stone powder
B	Sand (S1) $t=4$ mm, 6 mm, 8 mm, 10 mm, and 12 mm	JGT PGT	For determination of optimum thickness of sand layer S1
C	Sand (S2) $t=4$ mm, 6 mm, 8 mm, 10 mm, 12 mm, and 14 mm	JGT PGT	For determination of optimum thickness of sand layer S2
D	Sand (S3) $t=6$ mm, 8 mm, 10 mm, 12 mm, 14 mm, and 16 mm	JGT PGT	For determination of optimum thickness of sand layer S2

*t = thickness of sand layer

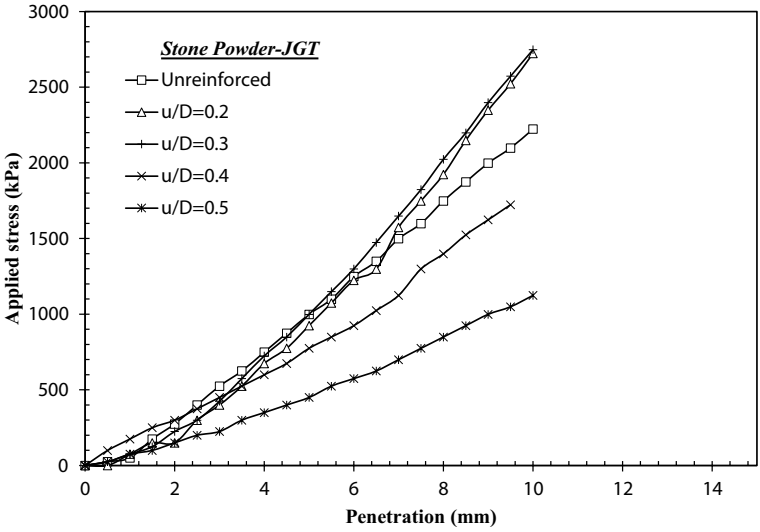

Fig. 5 Variation of stress-penetration of stone powder at different placement depths of JGT

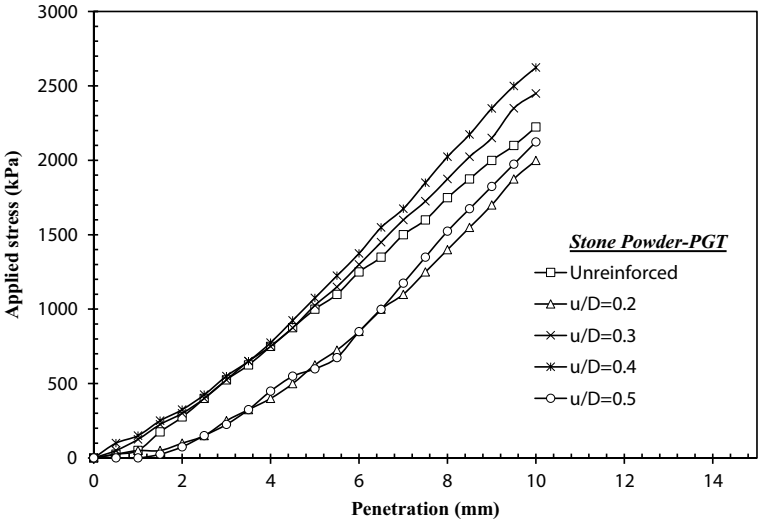

Fig. 6 Variation of stress-penetration of stone powder at different placement depths of PGT

of reinforcement (u). Based on Fig. 7, the improvement factor test results of JGT, it could be understood that the improvement factor is increasing from 0.2D to 0.3D; thereafter, the improvement factor is reduced for the settlements of 5 mm. It could happen due to the overburden pressure which acts at the position of reinforcement of 0.3D is sufficient to resist the loads up to its maximum. Hence, the results revealed that the optimum placement depth of the JGT reinforcement layer is 0.3D. Similarly,

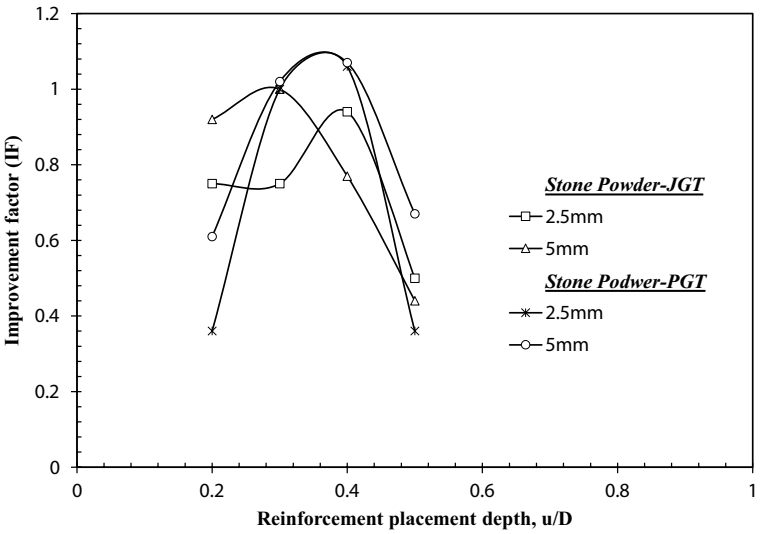

Fig. 7 Variation of improvement factor at different placement depths of JGT and PGT

the PGT reinforcement placement depth effect on the variation of improvement factors showed the optimum placement depth is 0.4D. It means that the PGT reinforcement needed higher overburden pressure to resist the loadings as compared to JGT reinforcement. It could be due to the lesser interface frictional properties of stone powder–PGT and lesser tensile stiffness of PGT reinforcement needing higher overburden depth as compared to stone powder–JGT (Tables 2 and 3).

Interestingly, irrespective of JGT- and PGT-reinforced soil conditions, the improvement factor for the lower and greater placement depths than of optimum is less than 1. It means that the unreinforced conditional state stone powder bears higher loads as compared to reinforced conditions. It could have occurred due to the improper mobilization of tensile strengths in the reinforcements at lesser overburden pressures; as a result, sufficient tensile stresses are not mobilized. Moreover, the interface frictional properties are lesser than the internal frictional properties of stone powder. Hence, the improvement factor is less than 1. Similarly, for the case of higher placement depths, the stiffness of the stone powder had reduced due to the reinforcement layer acting as a separator at higher placement depths (i.e., the depth where more than the major vertical stress increased).

3.2 Sandwich Condition

3.2.1 Sand: S1

This section details the test results of Series C which were performed on the sand-encapsulating geotextile as shown in Fig. 4b. Figures 8 and 9 represent the variation of load penetration of sandwich conditional JGT and PGT having sand layer thicknesses of 4 mm, 6 mm, 8 mm, 10 mm, and 12 mm. The corresponding variation of

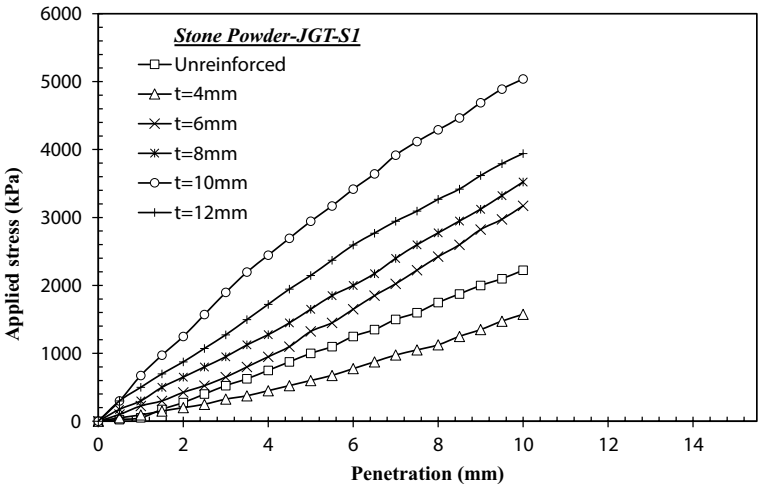

Fig. 8 Variation of stress-penetration of stone powder with JGT encapsulated different thicknesses of sand S1

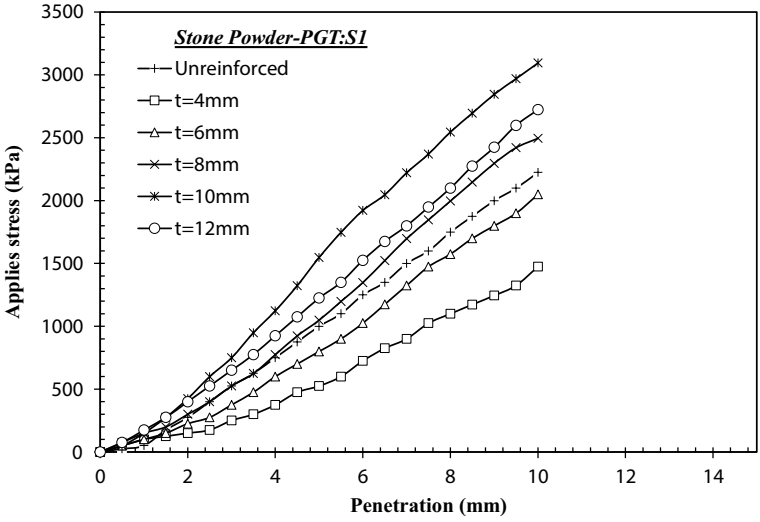

Fig. 9 Variation of stress-penetration of stone powder with PGT encapsulated different thicknesses of sand S1

the improvement factor with different sand layer thicknesses is depicted in Fig. 10. The test results revealed that the improvement factor increases with an increase in the thickness of the sand layer from 4 to 10 mm, irrespective of the type of reinforcement layer. Further increasing the thickness of 10 to 12 mm, the test results showed that the CBR load is diminished. Hence, it could be said that the optimum sand layer thickness for both the reinforcement cases of JGT and PGT is 10 mm.

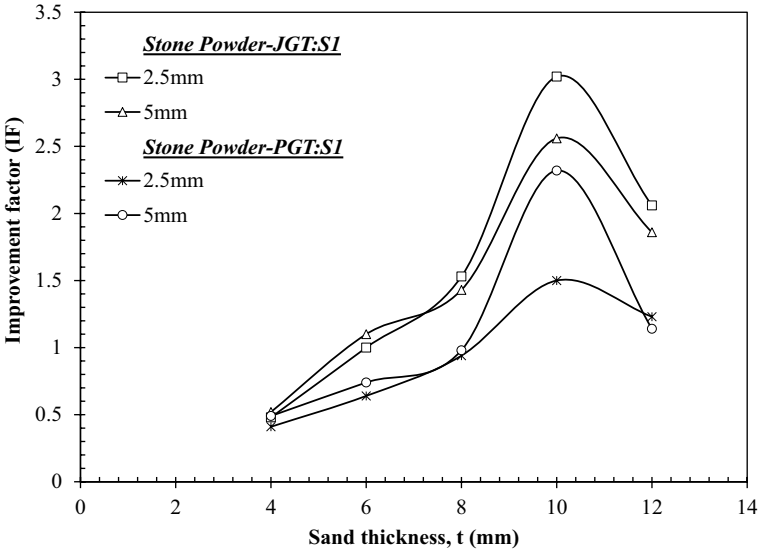

Fig. 10 Variation of improvement factor of JGT and PGT encapsulated various sand thicknesses of S1

Interestingly, the improvement factor for the sandwiched case of JGT and PGT is 3.02 times and 1.5 times higher at 2.5 mm, and 2.56 times and 2.32 times at 5 mm settlement as compared to the unreinforced conditions at an optimum sand layer thickness of 10 mm. It indicates that the JGT showed higher improvement as compared to PGT under the same optimum thickness of sand (i.e., 10 mm). It might have happened due to the high interface properties of JGT as per Table 3. Moreover, the JGT reinforcement material tears at the end of the test and it could happen due to the proper interactions and confinement of soil particles by the geotextile openings, and as a result the tensile stresses mobilize in the JGT reinforcement up to its ultimate. Moreover, as per Table 2, the tensile stiffness of JGT is 2.43 times higher as compared to PGT at same strain of 5%. Hence, the test results of sandwiched JGT performed well as compared to PGT under the same optimum thickness of sand.

3.2.2 Sand: S2

Series C tests were performed to see the effect of encapsulating sand layers (S2) of 4 mm, 6 mm, 8 mm, 10 mm, 12 mm, and 14 mm at the surfaces (top and bottom) of the JGT and PGT reinforcements. The corresponding improvement factor variation for both JGT and PGT with different sand layer thicknesses is depicted in Fig. 11. It could be said that the CBR load value enhanced with increasing the sand thickness from 4 to 10 mm for the case of JGT, and 4 to 12 mm for the case of PGT. In the case of JGT, the improvement factor for the sand layer thickness of 10 mm is optimum and 12 mm for the case of PGT. The higher thickness of optimum for the PGT occurred due to the variation of lesser

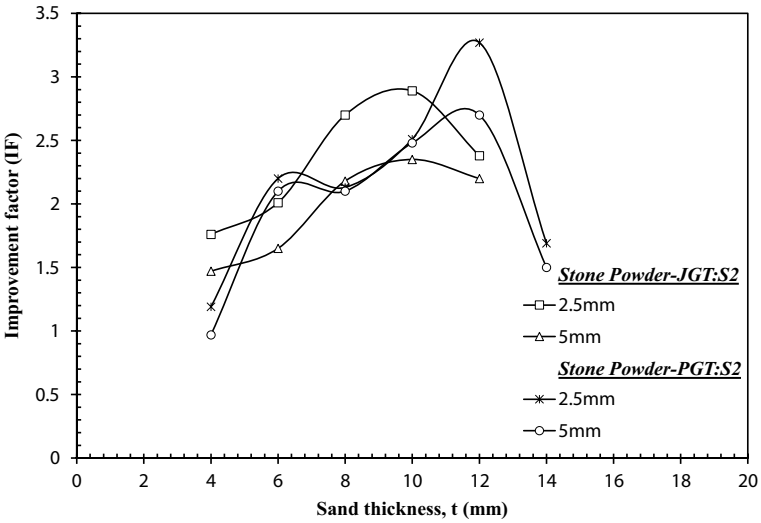

Fig. 11 Variation of improvement factor of JGT and PGT encapsulated various sand thicknesses of S2

interface frictional properties as compared to JGT mentioned in Table 3. Hence, the optimum thickness for the JGT and PGT could be considered 10 mm and 12 mm, respectively. The improvement factor for the sandwiched case of PGT and JGT is 3.2 times and 2.8 times higher as compared to the unreinforced conditions at optimum sand layer thicknesses, respectively. As per Table 3, even though the interface frictional properties for the case of PGT are lesser than JGT, the improvement factor for the case of PGT is 1.14 times higher than the JGT at the optimum sand layer thickness. It is contradictory as per the case of sandwich test results of sand S1. It might have happened due to the variation of sand particle size compared to the opening sizes of geotextile reinforcement material which quantifies the amount of soil confinement. For detailed evaluation, digital imaging techniques like particle image velocimetry (PIV) are needed (Venkateswarlu et al. 2023b). After finishing the test, the JGT sample does not tear as happened for the case of sandwich S1. It means that the tensile stresses are not fully developed in the sandwich condition S2-JGT as occurred in the case of the sandwich condition of S1-JGT. It might be due to variations in particle sizes and interactions of S1 and S2 with JGT reinforcement material.

3.2.3 Sand: S3

Series D shows the test results of the reinforced condition of stone powder with JGT and PGT reinforcements which are encapsulated with different sand layer (S3) thicknesses of 6 mm, 8 mm, 10 mm, 12 mm, 14 mm, and 16 mm. Figure 12 shows the variation of improvement factor of encapsulated different sand layer thicknesses of JGT and PGT reinforcements. The test results showed the improvement factor is increasing

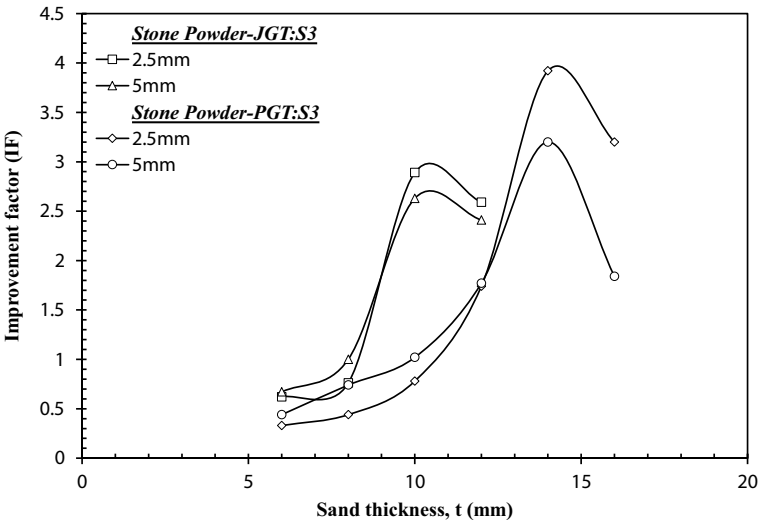

Fig. 12 Variation of improvement factor of JGT and PGT encapsulated various sand thicknesses of S3

with an increase in the sand layer thickness of up to 14 mm (for the case of PGT) and 10 mm (for the case of JGT). Interestingly, the optimum thickness is much varied for both the reinforcement cases which does not happen in the sandwich case of sands S1 and S2. It might have happened due to the larger variation of interface frictional properties of JGT and PGT as mentioned in Table 3. Notably, the optimum thickness for the case of PGT matched well with the test results of Unnikrishnan et al. (2002). It could happen due to the tensile stiffness of PGT and interface properties of S3-PGT

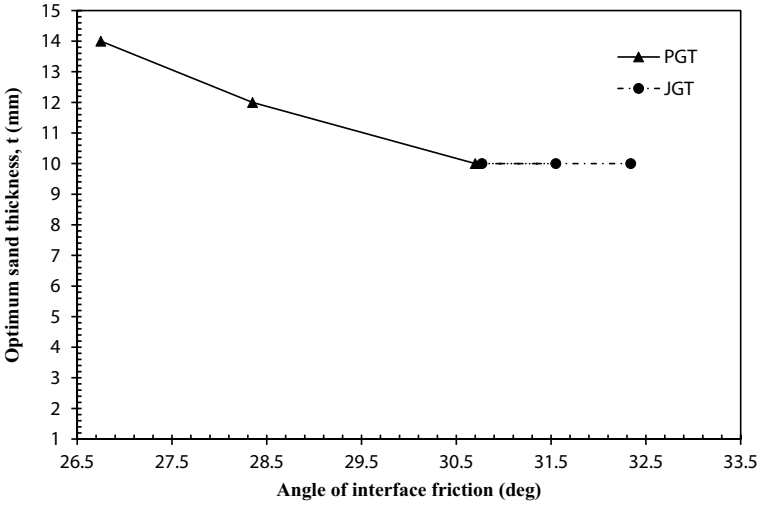

Fig. 13 Variation of optimum sand layers thickness (t) with respective Angle of interface frictional properties

of the present study are almost the same as Unnikrishnan et al. (2002). Finally, at the optimum sand layer thicknesses, the PGT showed 1.35 times and 1.21 times higher improvement factor as compared to JGT for both the settlements of 2.5 mm and 5 mm.

3.3 Comparison of Interface Frictional Properties (S1, S2, and S3)

Figure 13 depicts the influence of interface frictional properties on optimum sand layer thickness (t) for the case of encapsulating JGT and PGT. The variation of JGT and PGT interface frictional properties of S1, S2, and S3 and the corresponding optimum sand layer thickness (t) obtained from the CBR model tests is shown in Fig. 13. The test results show that the optimum sand layer thickness for the case of JGT is the same in all the test conditions. It might be due to the variation of interface frictional properties of sand-JGT is not much and hence the optimum thickness might be the same in all the cases of sands S1, S2, and S3. Interestingly, the case of PGT clearly states that the amount of optimum sand layer thickness is enhanced as interface frictional properties are reduced. In the reinforced soil structures, the shear stress generated from the actuating forces could be balanced or countered by the mobilized shear stresses at the soil-reinforcement interfaces. However, the mobilized shear stress would be decreased as moves away from the interfaces (Sridharan et al. 1991; Unnikrishnan et al. 2002). Therefore, a minimal thickness of extremely frictional material surrounding the reinforcement might be required more for the cases of lesser interface frictional conditions.

4 Conclusions

The following conclusions were drawn based on the present study

1) The optimum depths of the reinforcement layers in the stone powder which compacted at maximum dry unit weight and optimum moisture content were determined as 0.3D for the case of jute geotextile reinforcement layer (JGT) and 0.4D for the case of polypropylene geotextile reinforcement layer (PGT).
2) Irrespective of JGT and PGT, the optimum thickness of the sand layer in the case of sand S1 is 10 mm. Interestingly, the improvement with JGT is much higher as compared with PGT even though having the same optimum thickness of 10 mm. It could have happened due to the high tensile stiffness and interface properties of JGT as compared to PGT.
3) In the case of sand S2, the optimum sand layer thickness is determined as 10 mm and 12 mm for both the reinforcement cases of JGT and PGT. However, the improvement with PGT is 1.14 times higher as compared to JGT reinforcement under the same sand layer thickness.
4) The optimum thickness of sand layer S3 with JGT and PGT is 10 mm and 14 mm, respectively. The test results showed that the improvement with PGT is 1.35 times to 1.23 times higher than JGT at the respective optimum thickness of sand layers depending upon the settlement.

5) The test results of PGT reinforcement revealed that the optimum thickness of the sand layer depends upon the interface frictional properties of reinforcement layers.

5 Limitations

The limitations of the present study are detailed in this section as follows:

1) The difference in interface frictional properties of the sand-geotextile of the present study is not drastically varied. Hence, further model tests need to be performed by choosing the sand and geotextiles which consist of prominent variations of interface shear strength properties.
2) The present model tests are limited to CBR tests and lack the influence of interface frictional properties on optimum sand layer thickness under different confining pressures.
3) The present model tests are limited to geotextile reinforcements and unsoaked conditions only.

Author Contribution Eswara Reddy Orekanti conceptualized, designed, and carried out the experiments, analyzed the results, and contributed to writing the original draft preparation. Venkatesh Buragadda was instrumental during conceptualization, analysis, draft preparation, and reviewing. Sai Dharani Salammagari and Guru Swathi Vallepu contributed to carrying out the experiments and analyzing the results and contributed to writing and editing.

Data Availability All data, models, and code generated or used during the study appear in the published article.

Code Availability Not applicable.

Declarations

Ethics Approval and Consent to Participate Not applicable.

Consent for Publication Not applicable.

Competing Interests The authors declare no competing interests.

References

Abdi, M.R., Arjomand, M.A.: Pullout tests conducted on clay reinforced with geogrid encapsulated in thin layers of sand. Geotext. Geomembr. **29**(6), 588–595 (2011). https://doi.org/10.1016/j.geotexmem.2011.04.004

Abdi, M.R., Zandieh, A.R.: Experimental and numerical analysis of large scale pull out tests conducted on clays reinforced with geogrids encapsulated with coarse material. Geotext. Geomembr. **42**(5), 494–504 (2014). https://doi.org/10.1016/j.geotexmem.2014.07.008

Abdi, M.R., Sadrnejad, A., Arjomand, M.A.: Strength enhancement of clay by encapsulating geogrids in thin layers of sand. Geotext. Geomembr. **27**(6), 447–455 (2009). https://doi.org/10.1016/j.geotexmem.2009.06.001

ASTM D 1557–12: Standard test methods for laboratory compaction characteristics of soil using modified effort (56,000 ft-lbf/ft^3 (2,700 kN-m/m^3)). ASTM Int, West Conshohocken (2021)
ASTM D 1883–21: Standard test method for california bearing ratio (CBR) of laboratory-compacted soils. ASTM Int, West Conshohocken (2021)
ASTM D 4595–17: Standard test method for tensile properties of geotextiles by the wide-width strip method. ASTM Int, West Conshohocken (2017)
ASTM D 5199–12: Standard test method for measuring the nominal thickness of geosynthetics. ASTM Int, West Conshohocken (2012)
ASTM D 5261–10: Standard test method for measuring mass per unit area of geotextiles. ASTM Int, West Conshohocken (2018)
ASTM D6913: Standard test methods for particle-size distribution (gradation) of soils using sieve analysis. ASTM Int, West Conshohocken (2017)
ASTM D7928: Standard test method for particle-size distribution (gradation) of fine-grained soils using the sedimentation (hydrometer) analysis. ASTM Int, West Conshohocken (2021)
Bera, A.K., Ghosh, A., Ghosh, A.: Behaviour of model footing on pond ash. Geotech. Geol. Eng. **25**, 315–325 (2007). https://doi.org/10.1007/s10706-006-9112-5
Blayi, R.A., Sherwani, A.F.H., Mahmod, F.H.R., Ibrahim, H.H.: Influence of rock powder on the geotechnical behaviour of expansive soil. Int. J. Geosyn. Ground Eng. **7**, 1–13 (2021). https://doi.org/10.1007/s40891-021-00260-3
Buragadda, V., Thyagaraj, T., Dhiman, R., Orekanti, E.R., Maddileti, T.K.: Influence of geosynthetic reinforcement geometrical parameters on load-bearing capacity of sand: an experimental study. Transp. Infrastr. Geotech. 1–27 (2024). https://doi.org/10.1007/s40515-024-00416-4
Ghosh, A.: Compaction characteristics and bearing ratio of pond ash stabilized with lime and phosphogypsum. J. Mat. Civ Eng. **22**(4), 343–351 (2010). https://doi.org/10.1061/(ASCE)MT.1943-5533.0000028
Ghosh, A., Ghosh, A., Bera, A.K.: Bearing capacity of square footing on pond ash reinforced with jute-geotextile. Geotext. Geomembr. **23**(2), 144–173 (2005). https://doi.org/10.1016/j.geotexmem.2004.07.002
Kedar, H.N., Patel, S., Shirol, S.S.: Bulk utilization of steel slag–fly ash composite: a sustainable alternative for use as road construction materials. Innov. Infrastr. Sol. **9**(1), 21 (2024). https://doi.org/10.1007/s41062-023-01325-0
Latha, G.M., Venkateswarlu, H., Krishnaraj, P.: Science and technology of additive manufacturing applied to geotechnical engineering. Indian Geotech. J. **54**, 85–95 (2024). https://doi.org/10.1007/s40098-023-00777-6
Liu, X., Rong, Y., Chen, X., Chen, X., Zhang, W.: Recycling of waste stone powder in high fluidity grouting materials for geotechnical engineering reinforcement. Buildings **12**(11) (2022). https://doi.org/10.3390/buildings12111887
Pradhan, S.K., Pothal, G.K.: Experimental and cost evaluation of pond ash reinforced with polymeric geogrid. Multiscale Multidiscip. Model. Exp. Des. **7**(1), 349–363 (2024a). https://doi.org/10.1007/s41939-023-00214-4
Pradhan, S.K., Pothal, G.K.: Shear strength characteristics of pond ash reinforced with polymeric and natural fiber geosynthetic. Geotech. Geol. Eng. 1-22 (2024b).https://doi.org/10.1007/s10706-024-02765-w
Roy, R., Venkateswarlu, H., Hegde, A.: Numerical study on cyclic shear behavior of soil–geosynthetics interface. In: Sundaram, R., Shahu, J., Havanagi, V. (eds) Geotechnics for transportation infrastructure. Lecture Notes in Civil Engineering, vol 29. Springer, Singapore (2019). https://doi.org/10.1007/978-981-13-6713-7_19
Sarkar, R., Dawson, A.R.: Economic assessment of use of pond ash in pavements. Int. J. Pav. Eng. **18**(7), 578–594 (2015). https://doi.org/10.1080/10298436.2015.1095915
Sridharan, A., Murthy, B.S., Bindumadhava, Revanasiddappa, K.: Technique for using fine-grained soil in reinforced earth. J. Geotech. Eng. **117**(8), 1174–1190 (1991). https://doi.org/10.1061/(ASCE)0733-9410(1991)117:8(1174)
Teferra, T.E., Assefa, E., Assefa, S.M.: Influence of eggshell ash and stone powder on geotechnical properties of expansive clay in Dukem Town. Adv. Civ. Eng. **1**, 6690298 (2023). https://doi.org/10.1155/2023/6690298
Unnikrishnan, N., Rajagopal, K., Krishnaswamy, N.R.: Behaviour of reinforced clay under monotonic and cyclic loading. Geotext. Geomembr. **20**(2), 117–133 (2002). https://doi.org/10.1016/S0266-1144(02)00003-1

Venkateswarlu, H., Krishnaraj, P., Latha, G.M.: Three-dimensionally printed polypropylene sheets: insights on mechanical and interface shear behavior. J. Mat. Civ. Eng. **35**(9), 04023284 (2023a). https://doi.org/10.1061/JMCEE7.MTENG-15089

Venkateswarlu, H., SaiKumar, A., Latha, G.M.: Sand-geogrid interfacial shear response revisited through additive manufacturing. Geotext. Geomembr. **51**(4), 95–107 (2023b). https://doi.org/10.1016/j.geotexmem.2023.04.001

Yang, K.H., Yalew, W.M., Nguyen, M.D.: Behavior of geotextile-reinforced clay with a coarse material sandwich technique under unconsolidated-undrained triaxial compression. Int. J. Geomech. **16**(3) (2015). https://doi.org/10.1061/(ASCE)GM.1943-5622.0000611

Yetimoglu, T., Wu, J.T., Saglamer, A.: Bearing capacity of rectangular footings on geogrid-reinforced sand. J. Geotech. Eng. **120**(12), 2083–2099 (1994). https://doi.org/10.1061/(ASCE)0733-9410(1994)120:12(2083)

Yetimoglu, T., Inanir, M., Inanir, O.E.: A study on bearing capacity of randomly distributed fiber-reinforced sand fills overlying soft clay. Geotext. Geomembr. **23**(2), 174–183 (2005). https://doi.org/10.1016/j.geotexmem.2004.09.004

Authors and Affiliations

Eswara Reddy Orekanti[1,3] · Venkatesh Buragadda[1,2] · Sai Dharani Salammagari[1] · Guru Swathi Vallepu[1]

✉ Eswara Reddy Orekanti
orekantieswar@gmail.com

Venkatesh Buragadda
venkateshiitm15@gmail.com

Sai Dharani Salammagari
saidharanisalammagari@gmail.com

Guru Swathi Vallepu
guruswathi2002@gmail.com

[1] Department of Civil Engineering, School of Engineering, Mohan Babu University (Erstwhile Sree Vidyanikethan Engineering College), Tirupati, Andhra Pradesh 517102, India

[2] School of Civil and Environmental Engineering, Faculty of Engineering and Built Environment, University of the Witwatersrand, Johannesburg, South Africa

[3] Department of Civil Engineering, Sri Venkateswara College of Engineering (Autonomous), Tirupati, Andhra Pradesh 517507, India